Physical Chemistry Chemical Physics

ARTICLE

Microsolvation of Ethyl Carbamate Conformers: Effect of Carrier Gas on the Formation of Complexes.

Received 00th January 20xx,
Accepted 00th January 20xx

DOI: 10.1039/x0xx00000x

www.rsc.org/

Pablo Pinacho,[a,b] Juan Carlos López,*[a] Zbigniew Kisiel,[c] and Susana Blanco*[a]

Microsolvated complexes of ethyl carbamate (urethane) with up to three water molecules formed in a supersonic expansion have been characterized by high-resolution microwave spectroscopy. Both chirped-pulse and cavity Fourier transform microwave spectrometers covering the 2-13 GHz frequency range have been used. The structures of the complexes have been characterized and show water molecules closing sequential cycles through hydrogen bonding with the amide group. As is the case in the monomer, the ethyl carbamate-water complexes exhibit a conformational equilibrium between two conformers close in energy. The interconversion barrier between both forms has been studied by analyzing the spectra obtained using different carrier gas in the expansion. Complexation of ethyl carbamate with water molecules does not appear to significantly alter the potential energy function for the interconversion between the two conformations of ethyl carbamate.

1 Introduction

The carbamate group (-NCO_2-) is recurrent in many biologically active molecules with pharmacological applications.[1,2] The carbamate group can be considered as an ester-derivative of an amide, and therefore it offers some of the functionalities of the peptide bond. In consequence, the molecules presenting this group are used as peptide bond substitutes in medicinal chemistry.[2] One of the roles in which this functionality becomes important is in the possible modulation of inter- and intramolecular interactions with enzymes or molecular receptors. Carbamates may act as hydrogen bond donors or as hydrogen bond acceptors through the N-H or the C=O groups, respectively. This dual character, allows carbamates to form sequential cycles with other molecules having the same donor/acceptor character, as for example water molecules. The carbamate group also has wide applications in industry,[3] for example ethyl carbamate or urethane, has special importance in the polyurethane polymer synthesis.[4]

One of the reasons that the study of ethyl carbamate has sparked widespread interest is due to its presence in fermented food and wines.[5] Although its toxicity in humans is not clear, it is classified as a carcinogenic compound and consequently its concentration level is regulated by law. For this reason, various methods are being developed for their detection, aiming for quick and simple detection without laborious preparation processes. A new method, molecular rotational resonance (MRR),[6,7] based on rotational spectroscopy appears to be a useful alternative to classical methods, since it presents high precision and sensitivity. This technique requires prior knowledge of the rotational spectrum of the system to be detected, as well as of its intrinsic characteristics, such as the conformational equilibrium, or its interaction with other molecules present such as water, a universal solvent.

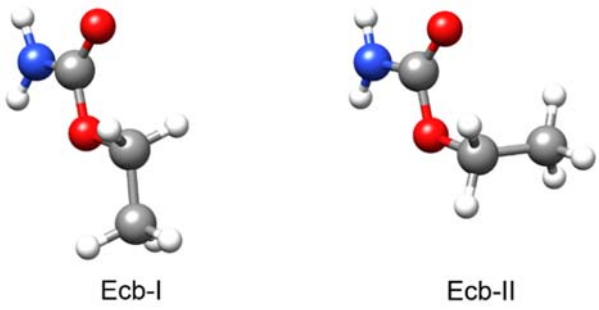

Figure 1. Experimentally observed conformations I and II for ethyl carbamate monomer.

[a] Dr. P. Pinacho, Prof. S. Blanco, Prof. J. C. López
Departamento de Química Física y Química Inorgánica, Facultad de Ciencias, Universidad de Valladolid, E-47011 Valladolid, Spain
E-mail: sblanco@qf.uva.es, jclopez@qf.uva.es
[b] Current address Deutsches Elektronen-Synchrotron, Notkestraβe 85, 22607, Hamburg, Germany
E-mail: pablo.pinacho@desy.de
[c] Prof. Z. Kisiel
Institute of Physics, Polish Academy of Sciences, Warsaw, Poland
E-mail: kisiel@ifpan.edu.pl

Electronic Supplementary Information (ESI) available: [complete calculation results and comparison with experimental values, Potential Energy Surfaces for the interconversion of ethyl carbamate, experimental structures, list of observed transitions frequencies]. See DOI: 10.1039/x0xx00000x

The structure of the ethyl carbamate (ecb) monomer has already been studied by different experimental techniques as X-ray crystallography,[8] IR spectroscopy in solid phase and in solution,[9] or microwave spectroscopy in the gas phase both at room temperature[10] and in supersonic expansion.[11] The gas phase studies confirmed the existence of two stable conformations very close in energy, in good agreement with the computational predictions. In ethyl carbamate I (ecb-I), the heavy atom backbone presents an effective planar configuration, while in ethyl carbamate II (ecb-II), the carbamate and the ethyl group are at an angle of approximately 80 degrees (see Figure 1). The second form is further stabilized by CH···O weak hydrogen bond, making it more stable than expected at first. For that reason, it was challenging to determine unambiguously which of the two forms is the most stable. Experimental investigations[10] estimated that ecb-I is more stable by 0.5(5) kJ·mol^{-1}. This was supported by theoretical calculations and experimental evidence, such as the absence of form II in supersonic expansion when Ar was used as the carrier gas.[10,11] Form II is also absent in the crystalline state[8], although it might be due to packaging effects in the crystal. The effect of carrier gas on conformational interconversion by means of collisional relaxation in supersonic jets has been widely studied.[12,13] Thus, different carrier gases can be used to select the conformers present in the jet, as happens in the equilibrated ethyl carbamate. Using Ne carrier gas both conformations can be observed, while using Ar conformer II is not detected, demonstrating the selective condensation to the energy lowest conformer on stronger cooling.

In this work, we aimed to characterize the hydrogen bond interactions between water and the peptide bond, evidenced by microsolvated complexes of molecules containing the amide group. Microsolvated complexes of ethyl carbamate can be considered as the next step in the understanding of microsolvated amides,[14-23] contributing information about the interactions of water with a substituted *cis*-peptide linkage, and on how water affects the linkage structure in the first steps of solvation. The study of the complexes of both forms of ethyl carbamate is expected to reveal the possible influence of solvation on the equilibrium conformations of this molecule. We have focused on the relaxation processes in the supersonic expansion of the species observed and their possible relation not only with the monomer dynamics, but also with the hydration degree. To achieve this, we have used high-resolution microwave spectroscopy combined with supersonic expansion, which allows generating the complexes in isolation conditions and characterization with high accuracy of their structure and properties.

2 Theoretical and experimental methods

Quantum-chemical calculations[24] were performed to study the preferred sites of interaction for both ethyl carbamate I and II conformations with water. Different structures were tested for the 1:1, 1:2 and 1:3 complexes (see Figures S1 and S3) based on the complexes previously reported for the microsolvation system of formamide,[14,18,20,21] or formanilide,[22] similar in functional chemistry group structures to ethyl carbamate. The geometries for the complexes were optimized using the B3LYP [25] functional combined with empirical dispersion correction (GD3)[26] and triple Z basis set 6-311++G(d,p)[27] or def2-TZVP.[28] In both cases, the results were almost identical. Frequencies using vibrational harmonic terms were also calculated to confirm that the optimized geometries are true minima. The energy values were refined by using the zero point energy (ZPE) correction. The calculated rotational constants, dipole moment components and nuclear quadrupole coupling constants allowed simulation of the microwave spectra for the different stable complexes. All the predicted parameters are collected in Tables S1 and S2. Calculations for the potential energy function for the interconversion between the rotamers I and II through ethyl or water movements were also performed using Density Functional Theory (DFT) and MP2/aug-cc-pVDZ methods in order to help in understanding the effect of the carrier gas on the relaxation and complexation (Figures S4 and S5).

The initial study of the microsolvated complexes of ethyl carbamate was carried out in the chirped-pulse Fourier transform microwave (CP-FTMW) spectrometer.[29,30] Ethyl carbamate is a white crystalline solid, commercially available, with melting point of *ca*. 57 ºC that was held in a stainless steel heatable pulsed nozzle and heated to about 80 ºC. Either Ar or Ne were used as carrier gas with backing pressures between 2-3 bar. The vapor from the sample was mixed with the carrier gas, previously seeded with water. Temperature and pressure were optimized to ensure maximum signal. The supersonic jet was generated by the expansion of the gas mixture through a small diameter (0.8 mm) nozzle into the high-vacuum chamber. The spectrum of ethyl carbamate was recorded from 2 to 8 GHz, using a chirped pulse of *ca*. 5 μs for the polarization of the sample. The frequency measurement accuracy is better than 10 kHz. Measurements in the 5-12 GHz frequency region were made in the narrow band molecular beam Fourier transform microwave (MB-FTMW) spectrometer.[31] Ethyl carbamate was placed in a small diameter (0.9 mm) stainless steel heating pulsed nozzle,[32] and heated to *ca*. 90 ºC, using Ar as carrier gas at backing pressures of about 2 bars. A short microwave pulse of *ca*. 2 μs at a discrete frequency is emitted, inducing the polarization of the sample over a narrow band of *ca*. 2 MHz. Due to the instrumental Doppler effect all the transitions appear split into two components. The transition frequency was calculated as the arithmetic mean of those Doppler components resulting in an accuracy of frequency measurement better than 3 kHz. The higher resolution power of this instrument allowed to fully resolve the hyperfine structure due to the nuclear quadrupole coupling and to determine precisely the diagonal elements of the quadrupole coupling tensor.

3 Results and discussion

Microwave spectra of ethyl carbamate I ··· $(H_2O)_n$ (n = 1, 2, 3) complexes

The microwave rotational spectrum was recorded in the CP-FTMW spectrometer[29,30] using Ar as carrier gas. After removing the lines corresponding to the ecb-I monomer, no evidence of ecb-II or of its complexes was observed. The lowest energy microsolvated complexes of ecb-I with up to three water molecules (see Figure 2) were easily identified by the observation of characteristic [a]R-branch groups of lines. For the ecb-I-w complex [b]R-branch and [b]Q-branch transitions were also observed. Preliminary rotational constants for ecb-I-w, ecb-I-w_2 and ecb-I-w_3 were initially derived from this spectrum.

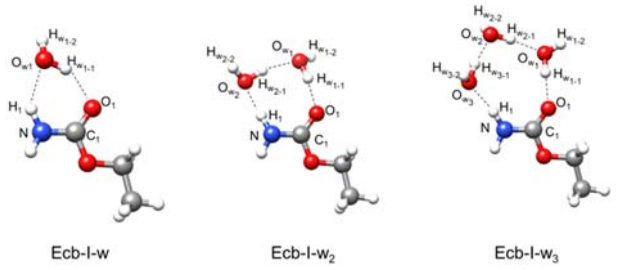

Figure 2. The complexes with one, two and three molecules of water with ethyl carbamate I.

Refined measurements in the narrow band MB-FTMW spectrometer[31,32] then allowed to completely resolve the nuclear quadrupole coupling hyperfine structure (hfs) present in all the spectra due the presence of a ^{14}N nucleus, and also an additional splitting in the lines of ecb-I-w_3 (see Figure 3). The MB-FTMW measurements lead to accurate determination of the rotational, quartic centrifugal distortion and nuclear quadrupole coupling constants.

No isotopologues in natural abundance were observed for any of the complexes, since each rotational transition appears spread over several hyperfine components decreasing its intensity (see Figure 3). The microwave spectra of ecb-I-w and ecb-I-w_2 monoisotopically substituted with ^{18}O in the water subunits were registered in the MB-FTMW spectrometer using a mixture of isotopically enriched $H_2{}^{18}O$ (99%) with normal water. That mixture was prepared with different $H_2{}^{16}O$:$H_2{}^{18}O$ proportions in order to ensure maximum probability of substitution of water molecule for each of the mono-, di- and trihydrated complexes. Selected transitions were measured to determine the rotational constants for the isotopic species. The spectra of ecb-I-w and ecb-I-w_2 species were analyzed using a semirigid-rotor Hamiltonian (A-reduction, I^r representation)[33,34] including quadrupole coupling terms employing the SPFIT/SPCAT program suite.[35]

For ecb-I-w_3, which displays the above mentioned vibrational doublets separated by about 0.018 - 0.020 MHz (see Figure 3), the centrifugal distortion constants and quadrupole coupling constants have been determined simultaneously for both states using a two-states Hamiltonian. The doublets do not show statistical weight spin effects, so those can in principle arise from a motion in the water subunit(s) connecting two equivalent forms. Similar doublets, but with larger separation, were observed for the formamide···$(H_2O)_3$ complex (f-w_3).[21] The hydrogen bond network established in ecb-w_3 is similar to that found in f-w_3,[21] being almost identical in the disposition of the water molecules. For that reason, it can be assumed that a path similar to that described for f-w_3 could be the origin of the doublets observed in ecb-I-w_3. The proposed path involves a coordinate movement of the water molecules, in which the consecutive flipping motions of each water molecule pass through reasonable low hindering barriers.[21] However, in the present case, since ecb is heavier than formamide, the energy difference between the ground and excited state should be smaller, while the small observed splitting magnitude is not sufficient to determine the energy difference between the states and the Coriolis constants. Only the rotational constants for each state were determined and are given in Table 3.

A search for other monohydrated complexes of the I form (see Figure S1), was carried out, however those complexes were not detected in our experimental conditions. The results for the parent species for the complexes of ecb-I with up to three molecules of water are collected and compared with quantum-chemically calculated values in Tables 1-3. The complete results, experimental frequencies and derived rotational parameters, are reported in SI.

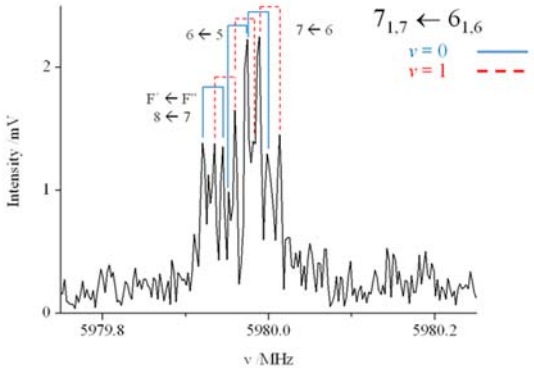

Figure 3. The $7_{1,7}$←$6_{1,6}$ rotational transition for the ecb-I-w_3 complex with the hyperfine structure arising from the quadrupole coupling interaction (F´←F´´ transitions). The small splittings of *ca*. 0.02 MHz correspond to the rotational transitions in the *v* = 0 (lower v, blue) and *v* = 1 (higher v, red) torsional states due to tunnelling between two equivalent configurations. Each transition appears as a doublet due to the instrumental Doppler effect.

Microwave spectra of ethyl carbamate II···$(H_2O)_n$ (n = 1, 2, 3) complexes

The microwave spectrum was also recorded with Ne carrier gas in the CP-FTMW spectrometer. In this spectrum, a greater density line can be observed, which turns out to correspond to the presence of both I and II forms of ethyl carbamate and of their water complexes. The mono, di and trihydrated complexes of ecb-II were identified in the microwave spectrum

by the recognition of [a]R-branch transition pattern. For the complex ecb-II-w some [b]R-branch and also [b]Q-branch transitions were detected. The observed ecb-II-w_n complexes (see Figure 4) present the same water arrangement, with identical interactions, as those observed for the ecb-I-w_n complexes. The only difference between the two sets of complexes comes from the different arrangement of the ethyl group in the two ecb rotamers.

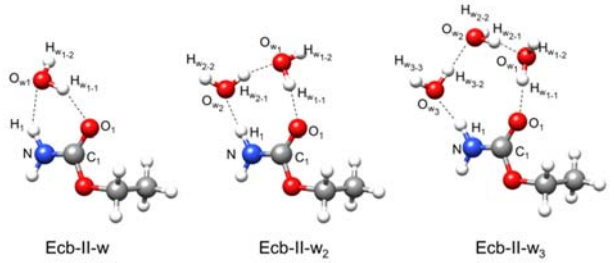

Figure 4. The complexes with one, two and three molecules of water with ethyl carbamate II.

A semirigid-rotor Hamiltonian[33,34] was used for the analysis of the spectra from the CP-FTMW. No isotopologues were observed for any of the complexes formed with ecb-II.

In the case of ecb-II, the complexes with water were predicted in pairs because some water atoms are out of the carbamate group plane (in conformers with w = 1,2 this concerns the hydrogens, for w = 3 also the water molecules). This plane coincides with the symmetry plane of ecb-I, and is the reason why ecb-I-w_n complexes have equivalent forms and the Interconversion between such forms can lead to splitting in rotational transitions, as has been stated in the trihydrated case. For ecb-II this is not possible because the ethyl chain breaks this symmetry, giving rise to two near equivalent conformers, that were labeled G+ or G- depending on the relative orientation of the ethyl chain with respect to water molecules (see Figure S2). The predicted data for all the conformers are compiled in the supplementary information.

The assignment was made by comparing the experimental constants with those calculated (B3LYP-GD3/6-311++G(d,p)) for each pair of predicted conformers for each complex. The assignment of ecb-II-w and ecb-II-w_2 complexes was difficult since the rotational parameters are quite similar, and appears that only the water OH bonds not involved in hydrogen bond change their orientation. The mono- and dihydrated complexes were assigned to conformer G- on the basis of the better agreement between experimental and calculated rotational constants and planar moments of inertia. The trihydrated complex assignment appears clearer and it was assigned to conformer G+ where the rotational parameters agree better for this conformer. As has been demonstrated in many cases,[36] the quadrupole coupling constants are very sensitive to the structural orientation, confirming the assignment to conformer G- for ecb-II-$w_{(1,2)}$ and G+ for ecb-II-w_3.

Table 1. Observed rotational parameters obtained for the ecb-I-w complex compared to B3LYP-GD3/6-311++G(d,p) values.

Parameter[a]	Experimental	Theoretical
A /MHz	7659.94791(44)[b]	7689.84
B /MHz	1034.10646(11)	1031.44
C /MHz	923.276293(93)	921.95
P_a /uÅ^2	485.05484(52)	486.21
P_b /uÅ^2	62.32085(52)	61.96
P_c /uÅ^2	3.65596(52)	3.76
Δ_J /kHz	0.1124(13)	0.098
Δ_{JK} /kHz	0.088(13)	-0.193
Δ_K /kHz	[0.][c]	22.061
δ_J /kHz	0.01594(58)	0.011
δ_K /kHz	[0.]	0.321
^{14}N 3/2(χ_{aa}) /MHz	2.4588(18)	2.72
^{14}N ¼(χ_{bb}-χ_{cc}) /MHz	1.60147(59)	1.81
n	138/37	
σ/kHz	2.4	

[a] *A*, *B* and *C* are the rotational constants. P_α (α = *a*, *b* or *c*) are the planar moments of inertia. Δ_J, Δ_{JK}, Δ_K, δ_J and δ_K are the quartic centrifugal distortion constants, χ_{aa}, χ_{bb} and χ_{cc} are the ^{14}N quadrupole coupling constants. *n* specifies the number of fitted hyperfine components and different rotational transitions. σ is the deviation of the fit. [b] Standard errors are given in parentheses in units of the last digit. [c] Parameters in square brackets were kept fixed.

Table 2. Observed rotational parameters obtained for the ecb-I-w_2 complex compared to B3LYP-GD3/6-311++G(d,p) values.

Parameter[a]	Experimental	Theoretical
A /MHz	3734.1586(72)	3793.57
B /MHz	701.90967(10)	704.09
C /MHz	597.04077(10)	599.88
P_a /uÅ^2	715.56974(31)	713.51
P_b /uÅ^2	130.90344(31)	128.96
P_c /uÅ^2	4.43601(31)	4.26
Δ_J /kHz	0.05569(31)	0.042
Δ_{JK} /kHz	0.2351(29)	0.161
Δ_K /kHz	[0.]	4.566
δ_J /kHz	0.01043(24)	0.007
δ_K /kHz	0.291(33)	0.264
^{14}N 3/2(χ_{aa}) /MHz	2.0278(58)	2.18
^{14}N ¼(χ_{bb}-χ_{cc}) /MHz	1.5582(57)	1.76
n	153/53	
σ/kHz	1.4	

[a] See Table 1 for definitions.

Table 3. Observed rotational parameters obtained for the ecb-I-w_3 complex compared to B3LYP-GD3/6-311++G(d,p) values.

	Experimental		Theoretical
Parameter[a]	v=0	v=1	
A /MHz	2254.4370(61)	2254.4248(61)	2260.09
B /MHz	486.842445(98)	486.843300(98)	493.14
C /MHz	410.026213(87)	410.027428(87)	413.03
P_a /uÅ^2	1023.22858(69)	1023.22523(69)	1012.40
P_b /uÅ^2	209.32433(69)	209.32402(69)	211.19
P_c /uÅ^2	14.84648(69)	14.84801(69)	12.42
Δ_J /kHz	0.08650(18)		0.062
Δ_{JK} /kHz	-1.104(10)		-0.595
Δ_K /kHz	[0.]		6.594
δ_J /kHz	0.01445(21)		0.010
δ_K /kHz	[0.]		0.217
3/2(χ_{aa}) /MHz	1.734(36)		1.79
¼(χ_{bb}-χ_{cc}) /MHz	1.4378(63)		1.38
n	180/30/30		
σ/kHz	2.0		

[a] See Table 1 for definitions.

Table 4. Observed rotational parameters obtained for the ecb-II-w complex compared to B3LYP-GD3/6-311++G(d,p) values.

Parameter[a]	Experimental	Theoretical – G-
A /MHz	5196.3808(28)	5109.80
B /MHz	1212.1730(10)	1220.31
C /MHz	1063.34957(89)	1067.74
P_a /uÅ^2	397.46735(26)	394.28
P_b /uÅ^2	77.80345(26)	79.04
P_c /uÅ^2	19.45251(26)	19.86
Δ_J /kHz	0.471(34)	0.392
Δ_{JK} /kHz	-2.35(14)	-3.545
Δ_K /kHz	[0.]	33.579
δ_J /kHz	0.076(13)	0.082
δ_K /kHz	[0.]	0.149
^{14}N 3/2(χ_{aa}) /MHz	2.3891(81)	2.70
^{14}N ¼(χ_{bb}-χ_{cc}) /MHz	1.2977(28)	1.38
n	54/16	
σ/kHz	6.6	

[a] See Table 1 for definitions.

Table 5. Observed rotational parameters obtained for the ecb-II-w_2 complex compared to B3LYP-GD3/6-311++G(d,p) values.

Parameter[a]	Experimental	Theoretical – G-
A /MHz	3023.593(94)	3060.95
B /MHz	797.6169(12)	802.41
C /MHz	672.6464(11)	676.37
P_a /uÅ^2	608.8977(27)	605.96
P_b /uÅ^2	142.4317(27)	141.24
P_c /uÅ^2	24.7135(27)	23.87
Δ_J /kHz	0.168(11)	0.132
Δ_{JK} /kHz	-0.942(62)	-0.561
Δ_K /kHz	[0.]	6.122
δ_J /kHz	0.064(16)	0.028
δ_K /kHz	[0.]	0.219
^{14}N 3/2(χ_{aa}) /MHz	2.001(12)	2.13
^{14}N ¼(χ_{bb}-χ_{cc}) /MHz	1.503(13)	1.69
n	51/18	
σ/kHz	5.5	

[a] See Table 1 for definitions.

Table 6. Observed rotational parameters obtained for the ecb-II-w_3 complex compared to B3LYP-GD3/6-311++G(d,p) values.

Parameter[a]	Experimental	Theoretical – G+
A /MHz	1885.263(24)	1899.24
B /MHz	557.96382(68)	568.28
C /MHz	458.15647(59)	462.15
P_a /uÅ^2	870.3792(19)	858.38
P_b /uÅ^2	232.6915(19)	235.16
P_c /uÅ^2	35.3766(19)	30.93
Δ_J /kHz	0.2207(32)	0.184
Δ_{JK} /kHz	-1.619(33)	-1.146
Δ_K /kHz	[0.]	5.477
δ_J /kHz	0.0392(37)	0.042
δ_K /kHz	[0.]	0.305
^{14}N 3/2(χ_{aa}) /MHz	1.900(50)	2.05
^{14}N ¼(χ_{bb}-χ_{cc}) /MHz	1.281(22)	1.34
n	76/27	
σ/kHz	6.0	

[a] See Table 1 for definitions.

However, it should be noted that these assignments are tentative, since the potential functions of these complexes have a very flat and broad minimum. The experimentally observed ground state is above the interconversion barriers to the water movements, so that the complexes present an average structure between all shallow minima.

No other conformers due to different water disposition were observed for any of these clusters. The experimentally determined rotational parameters are compared with the theoretically calculated ones in Tables 4-6. The complete data and results are collected in the SI.

Structure

As indicated by the relatively close values between predicted and determined rotational parameters (see Tables 1-6), the geometry from the results of quantum-chemical calculation can be considered, to a good approximation, to provide reliable description of the structure of all the complexes. The interactions established between ethyl carbamate, irrespective of its conformation, and water seems to be of the same nature as those reported before for complexes of related amides such as formamide,[14,18,21] N-methylformamide,[19] or formanilide.[22] For the monohydrated complexes, the water molecule interacts with the amide group closing a cycle through the $C_1{=}O_1{\cdots}H_{w1\text{-}1}{-}O_{w1}{\cdots}H_1{-}N$ hydrogen bond network (see Figures 2 and 4). The sequential cycle is extended in the complexes with two or three molecules of water through $C_1{=}O_1{\cdots}H_{w1\text{-}1}{-}O_{w1}{\cdots}H_{w2\text{-}1}{-}O_{w2}{\cdots}H_1{-}N$ and $C_1{=}O_1{\cdots}H_{w1\text{-}1}{-}O_{w1}{\cdots}H_{w2\text{-}1}{-}O_{w2}{\cdots}H_{w3\text{-}1}{-}O_{w3}{\cdots}H_1{-}N$ hydrogen bond networks respectively. In all cases, both ethyl carbamate and each water molecule act as hydrogen donor and hydrogen acceptor simultaneously.

Complexation with water does not seem to significantly alter the structure of the ethyl carbamate molecule. Thus, the complexes with the planar skeleton conformer ecb-I, are also close to planarity. It is possible to observe a steady increase in the experimental value of P_c from the monomer (3.332109(3) uÅ^2),[11] to ecb-I-w (3.6560(5) uÅ^2), and to ecb-I-w$_2$ (4.4360(3) uÅ^2) (see Tables 1 and 2), indicating the near planar nature of the complex heavy atom skeleton. The value of P_c in the hydrated complexes may include contributions from the out-of-plane hydrogen atoms of the ethyl group, from the water hydrogen atoms not involved in hydrogen bonding, and from vibrational contributions. The water oxygen nuclei in both complexes are located in the *ab* inertial plane, as indicated by the almost invariant value of P_c obtained for the $^{18}O_w$ isotopologues (see Tables S3 and S4). On moving to ecb-I-w$_3$ we note that its value of P_c increases considerably (14.8465(7) uÅ^2 for $v = 0$) (see Table 3). This indicates that the water molecules are positioned slightly out of the plane defined by the ecb-I conformer, as also has been observed in the similar complex f-w$_3$.[21]

For the ecb-II conformer (see Figure 2), the non-planarity of the monomer is also preserved in the complexes. Therefore, since the molecule has no plane of symmetry, the arrangement of the water molecules can not be directly related to the increase of the P_c planar moment. If we assume that, as in the ecb-I conformer, the water molecules lie in the pseudo plane of the carbamate group, we can consider that the methyl group is the main contributor to the P_c value. In this way, we have subtracted the contribution of the methyl group to each complex, so that the *ab* inertial plane coincides with the pseudo plane of the molecule, and therefore it is possible to analyze the new P_c values. The results are 0.6 uÅ^2 for ecb-II-w$_1$, 1.0 uÅ for ecb-II-w$_2$ and 9.1 uÅ for ecb-II-w$_3$, confirming that the water molecules lie on the carbamate plane, in a similar way to conformer ecb-I, keeping the same structure and interactions, even for the complex with three water molecules where the water molecules lie close to, but no longer on, the carbamate plane.

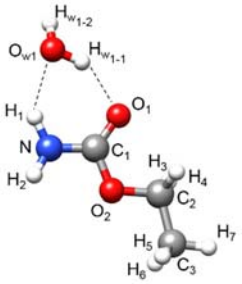

Fitted parameter	r_0	r_e
$r(O_{w1}\cdots H_1)$ /Å	2.0958(6)	2.079
$r(H_{w1\text{-}1}\cdots O_1)$ /Å	1.83(1)	1.913
$\angle(O_{w1}\cdots H_1{-}N)$ /°	137.66(3)	138.2
$\angle(H_{w1\text{-}1}\cdots O_1{-}C_1{-}N)$ /°	-181.5(1)	-175.2
Derived parameter	r_0	r_e
$r(O_{w1}{-}H_{w1\text{-}1})$ /Å	1.02(1)	0.975
$\angle(O_1{-}C_1{-}N)$ /°	125.100(8)	125.1
$\angle(H_1\cdots O_{w1}{-}H_{w1\text{-}1})$ /°	80.3(4)	81.5
$\angle(O_{w1}{-}H_{w1\text{-}1}\cdots O_1)$ /°	148.4(4)	148.5

	atom	*a*	*b*	*c*
$\lvert r_s\rvert$ /Å		3.4443(4)	0.351(4)	0.05(3)
r_0 /Å	O_w	3.4436(9)	-0.3657(7)	-0.0315(3)
r_e /Å		3.44	-0.35	-0.11

Figure 5. The derived r_0 structural parameters, the r_s coordinates and comparison with the r_e (B3LYP-D3/6-311++G(d,p)) structure for ecb-I-w.

For ecb-I-w and ecb-I-w$_2$ the monoisotopic $^{18}O_w$ substituted species were observed. For those complexes two procedures can be followed in order to obtain key parameters of the molecular structure: the so-called effective, r_0, or the substitution, r_s, method. The r_0 structure[37] reproduces the rotational constants in the ground state and is obtained by a least-squares fit of selected bond distances and angles to the observed rotational constants for all of the available isotopologues.[38] We have used the computed r_e results as starting point structure for the r_0 calculations. The r_0 structures obtained for the hydrogen bond parameters are summarized in Figures 5 and 6, where they are compared with the equilibrium r_e (B3LYP-GD3/6-311++G(d,p)) predicted structure. The complete results of r_0 structure determinations for ecb-I-w and ecb-I-w$_2$ are collected in Tables S9-S10. The r_s structure is based on the change of the values for the moments of inertia occurring upon monoisotopic substitution. It gives the

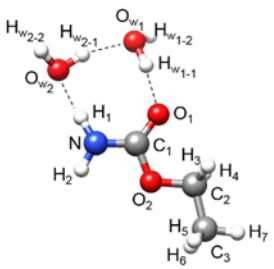

Fitted parameter	r_0	r_e
$r(O_{w2}\cdots H_1)$ /Å	1.887(7)	1.876
$r(H_{w1\text{-}1}\cdots O_1)$ /Å	1.778(1)	1.767
$\angle(O_{w2}\cdots H_1{-}N)$ /°	175.0(6)	174.1
$\angle(H_{w1\text{-}1}\cdots O_1{-}C_1)$ /°	129.5(3)	129.4
$\angle(H_{w1\text{-}1}\cdots O_1{-}C_1{-}O_2)$ /°	174.0(2)	176.5
Derived parameter	r_0	r_e
$r(H_{w2\text{-}1}\cdots O_{w1})$ /Å	1.836(5)	1.775
$r(O_{w2}\cdots O_{w1})$ /Å	2.763(5)	2.722
$\angle(O_{w2}{-}H_{w2\text{-}1}\cdots O_{w1})$ /°	160.3(5)	161.0
$\angle(H_{w2\text{-}1}\cdots O_{w1}{-}H_{w1})$ /°	98.6(2)	98.9

	atom	*a*	*b*	*c*
$\lvert r_s\rvert$ /Å		2.8133(5)	1.6251(9)	0.05(3)I
r_0 /Å	O_{w1}	2.813(1)	-1.6311(3)	0.024(2)
r_e /Å		2.82	-1.61	0.00
$\lvert r_s\rvert$ /Å		3.3733(4)	1.069(1)	0.06(3)
r_0 /Å	O_{w2}	3.374(1)	1.076(6)	0.041(1)
r_e /Å		3.36	1.06	0.05

r_s /Å		2.752(2)
r_0 /Å	$O_{w1}\text{-}O_{w2}$	2.763(5)
r_e /Å		2.722

Figure 6. The derived r_0 structural parameters, the r_s coordinates and comparison with the r_e (B3LYP-D3/6-311++G(d,p)) structure for ecb-I-w$_2$.

absolute values for the *a*, *b* and *c* coordinates of the substituted atom in the principal axis system by solving the Kraitchman equations.[39] The realistic uncertainties in the coordinates are quoted according to the Costain rule.[40] The r_s coordinates are compared with the r_0 and r_e values in Figures 5 and 6, where it is possible to see the good agreement between them, which confirms the proposed structures.

Potential energy function and relaxation

In the supersonic expansion using Ar, only rotamer I of ecb is observed, and therefore only its complexes are formed. In the supersonic expansion using Ne, both monomers and their complexes appear. The potential energy function for the interconversion of ethyl carbamate conformers can be defined by the rotation of the τ (C_1–O_2–C_2–C_3) dihedral angle. The potential energy function for this motion has been evaluated at the B3LYP-GD3/6-311++G(d,p) and MP2/aug-cc-pVDZ levels of theory (see Figures S4 and S5). Based on these predictions, it appears that water molecules do not significantly alter the energetics for the interconversion between the two forms of ethyl carbamate. Thus, the equilibrium analysis can be reduced to the relaxation of ethyl carbamate monomer. In the monomer potential function, the experimental global minimum corresponds to rotamer I, in which τ is 180 degrees. The theoretical calculations seem to miscalculate the minima energy, and predict conformer II to be lower in energy ($\Delta E_{ecbII\text{-}I,B3LYP}$ = -31 cm^{-1}) (see Figure S5), in disagreement with the experimental conclusions. However, those calculations pertain to the energy of the r_e structure, which is not the real situation. This can be corrected by calculating the Zero Point Energy, which gives the energy of the ground vibrational state, and predicts the minima energy in good agreement with experiment ($\Delta E\ ZPE_{ecbII\text{-}I,B3LYP}$ = 19 cm^{-1}).

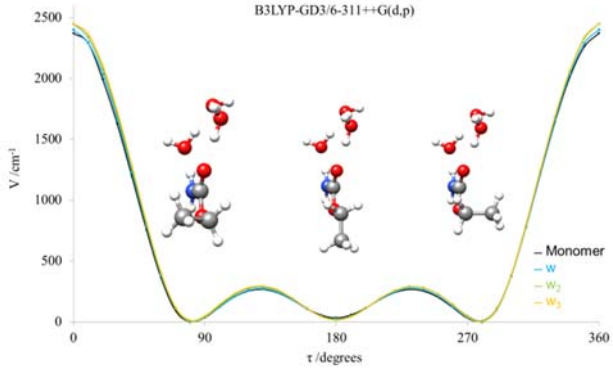

Figure 7. Potential energy function of ethyl carbamate performed at the B3LYP-D3/6-311++G(d,p) level of theory for the rotation of the τ (C_1–O_2–C_2–C_3) dihedral angle for the monomer (black) and the complexes with one (blue) two (green) or three (yellow) molecules of water. The corresponding structures at the minima are illustrated for the complex with three molecules of water in side view (See Figures S4 and S5 for more detail).

For the monomer, as a result of the almost planar heavy atom skeleton, an ethyl group rotation of +100 or -100 degrees from the global minimum leads to the two equivalent conformations of the II form. The periodic function at the B3LYP-GD3/6-311++G(d,p) level of theory predicts an energy barrier for the interconversion of about 290 cm^{-1}. This barrier is lower than the cutoff of 350 cm^{-1} established in the literature for conformer relaxation[12] in a molecular jet in the same conditions as we have used.

The barriers predicted for the complexes are similar to that of the monomer, even for ecb-II complexes, for which two different, almost isoenergetic, conformations may exist (G+ and G-). In ecb-II, the two similar forms of mono and dihydrated complexes arise from the symmetric and equivalent orientation of the non-bonded water hydrogen atoms that lie out of the carbamate plane, which become non-equivalent due to the different orientations of the ethyl group. For the ecb-II trihydrated complex, the arrangement of water molecules is not planar relative to the carbamate plane. As shown in Figure 7 for ecb-II-w_3, the two possible ecb-II forms which are equivalent for the monomer turn out to be non-equivalent for the complex, as in the other presently considered complexes. Experimentally only one of those conformations has been observed for the monohydrated, dihydrated or trihydrated ecb-II complexes. The conversion of the complex to the equivalent structure would require coordinated motions of both water and the ethyl group, over a surface with four minima where the conformers are equivalent in pairs. The interconversión barriers between all the rotamers through the coordinated movements are sufficiently low to allow the use of relaxation arguments to explain the non-observation of the missing conformers.[13]

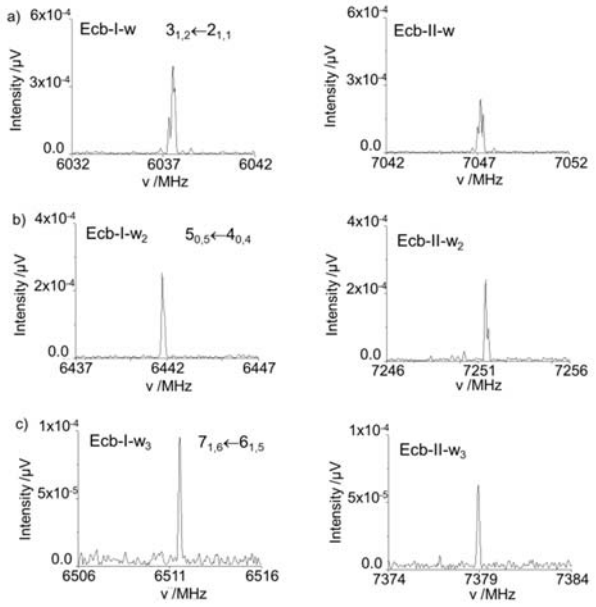

Figure 8. a) The $3_{1,2}$←$2_{1,1}$ rotational transition for the ecb-I-w and ecb-II-w complexes. b) The $5_{0,5}$←$4_{0,4}$ rotational transition for the ecb-I-w_2 and ecb-II-w_2 complexes. c) The $7_{1,6}$←$6_{1,5}$ rotational transition for the ecb-I-w_3 and ecb-II-w_3 complexes. All of the compared transitions were measured using the chirped pulse spectrometer in the same conditions of pressure (Ne at 3 bar) and sample heating temperature (75ºC).

It is possible to compare qualitatively the intensity of the same rotational transition for the complexes with one, two or three molecules of water with both forms of ethyl carbamate (see

Figure 8). As shown, the intensities are slightly lower for the complexes in ethyl carbamate II, but we can consider to a good degree of approximation that those are of the same order of magnitude. The populations in the supersonic jet can be estimated from the intensities in the chirped-pulse spectrum, assuming that the intensities are proportional to $N_i \cdot \mu_{i,\alpha}^2$, with N_i being the number density of the species *i* in the supersonic jet and $\mu_{i,\alpha}$ the electric dipole moment component allowing for the transition. Due to the close energy of both monomers, and the shape of the triple potential well, with two equivalent forms for ecb-II, the number density of molecules is expected to be 1:2 for ecb-I:ecb-II. Thus, rotational transitions of ecb-II and their complexes could be expected to be more intense, in opposition to the observed intensities.[41,42] Two effects can explain the discrepancy in the experimental intensities. The first is that the predicted dipole moment component is slightly larger for the complexes with ecb-I (see Tables S1 and S2). The second effect is that even using Ne, some partial relaxation process occurs, increasing the population of the ecb-I conformation.[41,42] Using Ar, all the ecb-II molecules relax due to collisions into the most stable form, which is ecb-I.

Nuclear quadrupole coupling and π-cooperative effects

σ-cooperativity[43,44] is associated with complexes in which there are groups capable of acting simultaneously as hydrogen donor and acceptor, closing cycles or forming chains. When water establishes hydrogen bonds, it polarizes incrementing the strength of the interactions further reflected by a shortening in the hydrogen bond distance. In addition to *σ*-cooperativity, another effect resulting in the polarization of the molecule can be expected for amides such as ethyl carbamate, which is Resonance Assisted Hydrogen Bonding (RAHB)[45,46] or *π*-cooperative bonding. Both *σ*- and *π*-cooperative effects become stronger as the number of water molecules increases. RAHB effects have been demonstrated to occur in the gas phase by using microwave spectroscopy for the microsolvation of formamide.[20,21] The main effect of RAHB on ethyl carbamate is its polarization, resulting in the enlargement of the C=O distance and the shortening of the C–N bond. No isotopologues in the ethyl carbamate molecule have been observed in this work, and therefore there is no direct experimental information about this effect. However, based on the good agreement between predicted and observed rotational parameters, the lack of experimental information can be supplemented by theoretical values as an approximation (see Scheme 1). The trend shown in the variation of the C = O and C-N bond distances confirms the existence of cooperative effects.

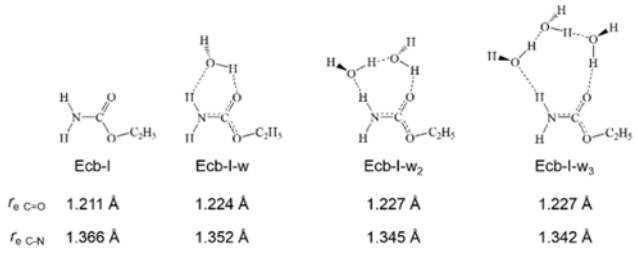

Scheme 1. RAHB inductive effects in the microsolvation series of ecb-I evidenced by the calculated C=O bond lengthening and the C–N bond shortening.

As already demonstrated in the microsolvation system of formamide,[20,21] the nuclear quadrupole coupling constants can be used to probe the changes in the electronic environment at the ^{14}N nucleus. In general, only the diagonal elements from the nuclear quadrupole coupling tensor can be determined and therefore an exhaustive picture of the electric field gradient can not be obtained. In planar molecules, the *c* inertial axis is parallel to the principal ^{14}N quadrupole coupling *z* axis. For near planar complexes, such as those observed with rotamer I of ethyl carbamate it is reasonable to assume $\chi_{cc} \approx \chi_{zz}$ correlation between quadrupole constants. Table S11 shows a clear tendency in the experimental values of χ_{cc} for the microsolvation series of ecb-I, which is almost identical to that found for formamide-water complexes.[20,21] The complexes with ecb-II are far from planarity, and therefore this correlation is not valid.

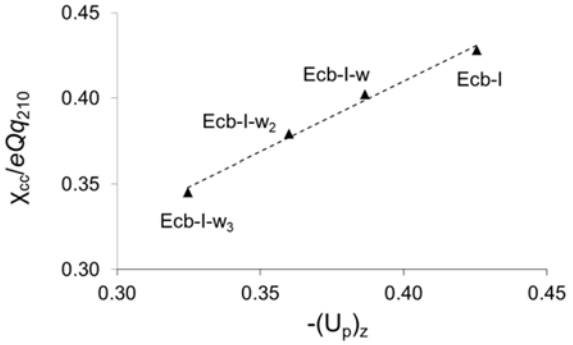

Figure 9. Correlation between the experimental values of χ_{cc}/eQq_{210} and $-(U_p)_z$ for the monomer and observed complexes of ethyl carbamate I with up to three water molecules. See the text and Table S11 for definition of the plotted quantities.

The trend in ecb-I indicates that the electronic environment at the ^{14}N nucleus is altered by microsolvation. The electric field gradient coupling to nuclear quadrupole can be related to the unequal filling of the valence shell *p* orbitals from the coupling nucleus.[33] The χ_{zz} constant can then be correlated to the unbalanced $2p_z$ electronic charge $-(U_p)_z$. Figure 9 shows the correlation between the experimental χ_{cc}/eQq_{210} and $-(U_p)_z$ calculated from a Natural Bond Orbital analysis.[47] It is possible to observe a good, almost linear, correlation for the values of ecb-I-w_n.

The $-(U_p)_z$ values indicate that the electron density along the *z* axis decreases with the hydration degree, showing that the polarization of ethyl carbamate due to RAHB inductive effects becomes stronger when the number of cooperative hydrogen bonds increases. When considering the diagonal quadrupole coupling tensor elements the predicted values of χ_{zz} are practically the same in both series of ecb-I and ecb-II complexes (see Table S11 and S12). This indicates that practically the same RAHB effects can be expected in the amide group, independently of the ethyl carbamate conformation.

4 Conclusions

Microsolvated complexes of ethyl carbamate with up to three molecules of water have been observed for the first time in the gas phase by high-resolution microwave spectroscopy. The observation of $H_2{}^{18}O$ species has allowed to precisely locating the water molecules in the molecular frame. The hydrogen bond distances obtained using the r_0 methodology indicate that the dominant interaction is, as already observed in related systems, the C=O···H_w–O_w. In the gas phase, ethyl carbamate presents equilibrium between two close energy conformations separated by a low interconversion barrier. The detection of these structures and of their microsolvated complexes depends strongly on the carrier gas used in the supersonic expansion and the associated relaxation processes. Using Ar, only the most stable form of ethyl carbamate and its water complexes are observable (ecb-I and ecb-I-w_n, n = 1-3), while using Ne, both ethyl carbamate forms and their hydrated complexes could be detected with comparable line intensities due to partial relaxation. It is noticeable that the inclusion of water molecules does not seem to alter the potential energy function for the interconversion between the two forms of ethyl carbamate. Although theoretical calculations miscalculate the relative energy order of the complexes due to the very small energy differences, the observation of only the complexes with ecb-I in the supersonic expansion using Ar indicates that those are more stable, and the ecb-II rotamers relax into them. A decreasing trend in the experimental value of χ_{cc}/eQq_{210} has been found as the number of water molecules in the ecb-w complexes increases, in similarity to other studies of microsolvated amides. RAHB inductive effect seems to be at the origin of this trend, that causes the elongation of the ethyl carbamate C=O bond distance while shortening the C–N bond distance. This has been shown to occur for both microsolvation series of ethyl carbamate.

Conflicts of interest

Authors declare that there are no conflicts of interest.

Acknowledgments

The authors acknowledge the Ministerio de Economía y Competitividad (Grant CTQ2016-75253-P) and the Junta de Castilla y León (Grant VA334U14) for financial support.

References

[1] Abraham, D. J., Rotella, D. P. *Burger´s medicinal chemistry, drug discovery and development*, 7th edition, Wiley, Hoboken, 2010.

[2] Ghosh, A. K., Brindisi, M. "Organic Carbamates in Drug Design and Medicinal Chemistry" *J. Med. Chem.*, **2015**, 58, 2895–2940.

[3] Fukuto, T. R. "Mechanism of Action of Organophosporus and Carbamate Insecticides" *Environ. Health Perspect.*, **1990**, 87, 245–254.

[4] Heyn, R. H., Jacobs, I. Carr, R. H. "Synthesis of Aromatic Carbamates from CO_2: Implications for the Polyurethane Industry" *Adv. Inorg. Chem.*, **2014**, 66, 83–115.

[5] Gowd, S., Su, H., Karlowski, P., Chen, W. "Ethyl Carbamate: An Emerging Food and Environmental Toxicant. *Food Chem.,* **2018**, 248, 312–321.

[6] Christophe, A. L.; Barnes, J. T.; Twagirayezu, S.; Mikhonin, A.; Muckle, M. T.; Neill, J. L. "Direct Measurements of Small Polar Impurities in Gasoline Mixtures Using Molecular Rotational Resonance Spectroscopy" *Appl. Spectrosc.*, **2019**, 73, 1334–1339.

[7] Armstrong, D. W.; Talebi, M.; Thakur, N.; Wahab, M. F.; Mikhonin, A. V.; Muckle, M. T.; Neill, J. L. "A Gas Chromatography-Molecular Rotational Resonance Spectroscopy Based System of Singular Specificity" *Angew. Chemie Int. Ed.*, **2020**, 59, 192–196.

[8] Bracher, B. H., Small, R. W. H. "The Crystal Structure of Ethyl Carbamate" *Acta Crystallogr.*, **1967**, 23, 410–418.

[9] Furer, V. L. "Hydrogen Bonding in Ethyl Carbamate Studied by IR Spectroscopy" *J. Mol. Struct.*, **1998**, 449, 53–59.

[10] Marstokk, K. M., Møllendal, H. "Microwave Spectrum, Conformational Equilibrium and Quantum Chemical Calculations of Urethane (Ethyl Carbamate)" *Acta Chem. Scan.*, **1999**, 53, 329–334.

[11] Goubet, M., Motiyenko, R. A., Réal, F., Margulès, L., Huet, T. R., Asselin, P., Soulard, P., Krasnicki, A., Kisiel, Z., Alekseev, E. A. "Influence of the Geometry of a Hydrogen Bond on Conformational Stability: A Theoretical and Experimental Study of Ethyl Carbamate" *Phys. Chem. Chem. Phys.*, **2009**, 11, 1719–1728.

[12] Ruoff, R. S., Klots, T. D., Emilsson, T., Gutowsky, H. S. "Relaxation of Conformers and Isomers in Seeded Supersonic Jets of Inert Gases" *J. Chem. Phys.*, **1990**, 93, 3142–3150.

[13] Godfrey, P. D., Brown, R. D., Rodgers, F. M. "The Missing Conformers of Glycine and Alanine: Relaxation in seeded Supersonic Jets" *J. Mol. Struct.*, **1996**, 376, 65–81.

[14] Lovas, F. J., Suenram, R. D., Fraser, G. T., Gillies, C. W., Zozom, J. "The microwave Spectrum of Formamide-Water and Formamide-Methanol Complexes" *J. Chem. Phys.*, **1988**, 88, 722–729.

[15] Maris, A., Ottaviani, P., Caminati, W., "Pure rotational spectrum of 2-pyridone···water and quantum chemical calculations on the tautomeric equilibrium 2-pyridone···water/2-hydroxypyridine···water" *Chem. Phys. Lett.,* **2002**, 360, 155–160.

[16] Lavrich, R. J., Tubergen, M. J., "Conformation and Hydrogen Bonding in the Alaninamide−Water van der Waals Complex" *J. Am. Chem. Soc.*, **2000**, 122, 2938–2943.

[17] Held, A., Pratt, D. W. "Hydrogen Bonding in Water Complexes. Structures of 2-Pyridone-H_2O and 2-Pyrididone-$(H_2O)_2$ in Their S_0 and S_1 Electronic States" *J. Am. Chem. Soc.*, **1993**, 115, 9708–9717.

[18] Blanco, S., López, J. C., Lesarri, A., Alonso, J. L. "Microsolvation of Formamide: A Rotational Study" *J. Am. Chem. Soc.*, **2006**, 128, 12111–12121.

[19] Caminati, W., López, J. C., Blanco, S., Mata, S., Alonso, J. L. "How Water Links to *Cis* and *Trans* Peptidic Groups: The rotational Spectrum of N-Methylformamide-Water" *Phys. Chem. Chem. Phys.*, **2010**, 12, 10230–10234.

[20] Blanco, S., Pinacho, P., López, J. C. "Hydrogen-Bond Cooperativity in $Formamide_2$-Water: A Model for Water Mediated Interactions" *Angew. Chem. Int. Ed.*, **2016**, 128, 9477–9481.

[21] Blanco, S., Pinacho, P., López, J. C. "Structure and Dynamics in Formamide-$(H_2O)_3$: A Water Pentamer Analogue" *J. Phys. Chem. Lett.*, **2017**, 8, 6060–6066.

[22] Pinacho, P., Blanco, S., López, J.C. "The complete conformational panorama of formanilide–water complexes: the role of water as a

conformational switch", Phys. Chem. Chem. Phys. **2019**, 21, 2177–2185.

[23] Pinacho, P., López, J.C., Kisiel, Z., Blanco, S. "Structure of Butyl Carbamate and of Its Water Complex in the Gas Phase" *J. Phys. Chem. A*, **2019**, 123, 7983–7990.

[24] Gaussian 09, Revision D.01, Frisch M. J., Trucks G. W., Schlegel H. B., Scuseria G. E., Robb M. A., Cheeseman J. R., Scalmani G., Barone V., Petersson G. A., Nakatsuji H., Li X., Caricato M., Marenich A., Bloino J., Janesko B. G., Gomperts R., Mennucci B., Hratchian H. P., Ortiz J. V., Izmaylov A. F., Sonnenberg J. L., Williams-Young D., Ding F., Lipparini F., Egidi F., Goings J., Peng B., Petrone A., Henderson T., Ranasinghe D., Zakrzewski V. G., Gao J., Rega N., Zheng G., Liang W., Hada M., Ehara M., Toyota K., Fukuda R., Hasegawa J., Ishida M., Nakajima T., Honda Y., Kitao O., Nakai H., Vreven T., Throssell K., Montgomery, Jr. J. A., Peralta J. E., Ogliaro F., Bearpark M., Heyd J. J., Brothers E., Kudin K. N., Staroverov V. N., Keith T., Kobayashi R., Normand J., Raghavachari K., Rendell A., Burant J. C., Iyengar S. S., Tomasi J., Cossi M., Millam J. M., Klene M., Adamo C., Cammi R., Ochterski J. W., Martin R. L., Morokuma K., Farkas O., Foresman J. B., Fox D. J., *Gaussian, Inc., Wallingford CT*, 2016.

[25] a) Lee, C., Yang, W., Parr, R. G. "Development of the Colle-Salvetti Correlation-Energy Formula into a Functional of the Electron Density" *Phys. Rev. B*, **1988**, 37, 785–789. b) Becke, A. D. "Density-Functional Thermochemistry. III. The Role of Exact Exchange" *J. Chem. Phys.*, **1993**, 98, 5648–5652. c) Vosko, S. H., Wilk, L., Nusair, M. "Accurate Spin-Dependent Electron Liquid Correlation Energies for Local Spin Density Calculations: a Critical Analysis" *Can. J. Phys.*, **1980**, 58, 1200–1211.

[26] Grimme, S., Antony, J., Ehrlich, Krieg, H. "A Consistent and Accurate *Ab Initio* Parametrization of Density Functional Dispersion Correction (DFT-D) for the 94 Elements H-Pu" *J. Chem. Phys.*, **2010**, 132, 154101.

[27] Ditchfield, R., Hehre, W. J., Pople, J. A. "Self-Consistent Molecular-Orbital Methods. IX. An Extended Gaussian-Type Basis for Molecular-Orbital Studies of Organic Molecules" *J. Chem. Phys.*, **1971**, 54, 724–728.

[28] Weigend, F., Ahlrichs, R. "Balanced basis sets of split valence, triple zeta valence and quadruple zeta valence quality for H to Rn: Design and assessment of accuracy" *Phys. Chem. Chem. Phys.*, **2005**, 7, 3297–3305.

[29] Brown, G. G., Dian, B. C., Douglass, K. O., Geyer, S. M., Pate, B. H. "The Rotational Spectrum of Epifluorohydrin Measured by Chirped-Pulse Fourier Transform Microwave Spectroscopy" *J. Mol. Spectrosc.*, **2006**, 238, 200–212.

[30] Brown, G. G., Dian, B. C., Douglass, K. O., Geyer, S. M., Shipman, S. T., Pate, B. H. "A Broadband Fourier Transform Microwave Spectrometer Based on Chirped Pulse Excitation" *Rev. Sci. Instrum.*, **2008**, 79, 053103.

[31] Alonso, J. L., Lorenzo, F. J., López, J. C., Lesarri, A., Mata, S., Dreizler, H. "Construction of a Molecular Beam Fourier Transform Microwave Spectrometer Used to Study the 2,5-Dihydrofuran-Argon Van Der Waals Complex" *Chem. Phys.*, **1997**, 218, 267–275.

[32] Blanco, S., López, J. C., Alonso, J. L., Ottaviani, P., Caminati, W. "Pure Rotational Spectrum and Model Calculations of Indole-Water" *J. Chem. Phys.*, **2003**, 119, 880–886.

[33] Gordy, W., Cook, R. L. *Microwave Molecular Spectra*, Wiley-Interscience, New York, 1984.

[34] Watson, J. K. G. in *Vibrational Spectra and Structure a Series of Advances, Vol 6* ed. J. R. Durig, Elsevier, New York, 1977, pp. 1–89.

[35] Pickett, H. M. "The Fitting and Prediction of Vibrational-Rotation Spectra with Spin Interaction" *J. Mol. Spectrosc.*, **1991**, 148, 371–377.

[36] Blanco, S., Lesarri, A., López, J.C., Alonso, J.L., "The Gas Phase Structure of Alanine" *J. Am. Chem. Soc.*, **2004**, 126, 11675–11683.

[37] Rudolph, H. D. "Contribution to the Systematics of r_0-Derived Molecular Structure Determinations from Rotational Parameters" *Struct. Chem.*, **1991**, 2, 581–588.

[38] Kisiel, Z. "Least-Squares Mass-Dependence Molecular Structures for Selected Weakly Bound Intermolecular Clusters" *J. Mol. Spectrosc.*, **2003**, 218, 58–67.

[39] Kraitchman, J. "Determination of Molecular Structure from Microwave Spectroscopic Data" *Am. J. Phys.*, **1953**, 21, 17–24.

[40] Costain, C. C. "Further Comments on the Accuracy of r_s Substitution Structures" *Trans. Am. Crystallogr. Assoc.*, **1966**, 2, 157–164.

[41] López, J. C., Macario, A., Blanco, S., "Conformational equilibria in o-anisic acid and its monohydrated complex: the prevalence of the trans-COOH form", *Phys. Chem. Chem. Phys.*, **2019**, 21, 6844–6850.

[42] Macario, A., Blanco, S., Thomax, J., Xu., J., López, J.C., "Competition between Intra- and Intermolecular Hydrogen Bonding: o-Anisic Acid ··· Formic Acid Heterodimer" *Chem. Eur. J.*, **2019**, 25, 12325–12331.

[43] Saenger, W., Jeffrey, G. A. *Hydrogen Bonding in Biological Structures*, Springer-Verlag, Berlin, 1991.

[44] Jeffrey, G. A. *Introduction to Hydrogen Bonding*, Oxford University Press, Oxford, 1997.

[45] Jeffrey, G. A. *An Introduction to Hydrogen Bonding*; Topics in Physical Chemistry - Oxford University Press, Oxford University Press, 1997.

[46] Gilli, P., Bertolasi, V., Ferretti, V., Gilli, G. "Evidence for Intramolecular N-H···O Resonance Assisted Hydrogen Bonding in *β*-Enaminones and Related Heterodienes. A Combined Crystal-Structural, IR, and NMR Spectroscopic, and Quantum-Mechanical Investigation" *J. Am. Chem. Soc.*, **2000**, 122, 10405–10417.

[47] Reed, A. E., Weinstock, R. B., Weinhold, F. "Natural Population Analysis" *J. Chem. Phys.* **1985**, *83*, 735–746.

